Boletín Geológico

Boletín Geológico, 52(2), 2025

https://revistas.sgc.gov.co/index.php/boletingeo

SERVICIO GEOLÓGICO COLOMBIANO

Research article

Tracing Neotropical springs in crystalline rocks: Hydrogeochemical and statistical insights

Rastreando manantiales neotropicales en rocas cristalinas: perspectivas hidrogeoquímicas y estadísticas

Laura **Chavarría-Arboleda**[1], Marcela **Jaramillo**[1]

[1]School of Applied Sciences and Engineering, Universidad Eafit, Medellín, Colombia

ABSTRACT

Historically, spring's hydrogeological, ecosystemic, and cultural importance has been recognized for protecting groundwater and surface water resources. However, in Colombia, studies on spring water are minimal, and there is no established methodology for their correct classification, especially in tropical zones, where the hydrogeological systems are highly complex due to abrupt topography, high precipitation, and the development of thick soils.

The primary objective of this study was to elucidate the interactions of rainwater and hydrochemical processes as it infiltrates, flows, and interacts with the underground medium in a mountainous area of the municipality of San Roque, Department of Antioquia, to determine whether the emerging water on the surface is groundwater or vadose water. For this purpose, hydrogeochemical analyses and multivariate clustering were conducted within the context of the area's hydrogeological knowledge, using on-site physicochemical and water quality data from various water types.

The results show that not all sampling points in the study zone can be classified as spring water; some exhibit a direct relationship with rainwater, without necessarily discharging from the saturated zone. Our results provide a preliminary assessment of the research and classification of spring waters in Colombia, which is crucial for refining current guidelines on the declaration of protected zones and on soil utilization associated with the groundwater resources.

Keywords: Vadose water, hydrometeorological interactions, tropical hydrogeology, hydrogeochemical characterization, multivariate analysis, mountain aquifer systems, groundwater

RESUMEN

Históricamente, se ha reconocido la importancia hidrogeológica, ecosistémica y cultural de los manantiales para proteger las aguas subterráneas y superficiales. Sin embargo, en Colombia los estudios sobre el agua de manantial son escasos y no existe una metodología establecida para su correcta clasificación, especialmente en zonas tropicales, donde los sistemas hidrogeológicos son altamente complejos debido a la topografía abrupta, las altas precipitaciones y el desarrollo de suelos gruesos.

El objetivo principal de este estudio fue dilucidar las interacciones del agua de lluvia y los procesos hidroquímicos a medida que esta se infiltra, fluye e interactúa con el medio subterráneo en una zona montañosa del municipio de San Roque, Departamento de Antioquia, para determinar si el agua que emerge en la superficie es subterránea o vadosa. Para este propósito, se realizaron análisis hidrogeoquímicos y estadísticas de agrupación multivariada, en el contexto del conocimiento hidrogeológico del área, utilizando datos in situ fisicoquímicos y de calidad de distintos tipos de agua.

Los resultados muestran que no todos los puntos de muestreo identificados en la zona de estudio pueden clasificarse como agua de manantial; algunos presentan una relación directa con el agua de lluvia sin necesariamente descargar de la zona saturada. Nuestros resultados proporcionan una evaluación preliminar de la investigación y la clasificación de las aguas de manantial en Colombia, lo cual es crucial para afinar los lineamientos actuales sobre la declaración de zonas protegidas y la utilización del suelo asociada al recurso de agua subterránea.

Palabras clave: agua vadosa, interacciones hidrometeorológicas, hidrogeología tropical, caracterización hidroquímica, análisis multivariado, sistemas acuíferos montañosos, agua subterránea.

Citación: Chavarría-Arboleda, L., Jaramillo, M., (2025). Tracing Neotropical springs in crystalline rocks: Hydrogeochemical and statistical insights. *Boletín Geológico*, 52(2). DOI: https://doi.org/10.32685/0120-1425/bol.geol.52.2.2025.759

Boletín Geológico: ISSS: printed; 0120-1425, ISSN electronic: 2711-1318.

Manuscript received: July 14, 2025; Review received: November 11, 2025; manuscript accepted: November 14, 2025

1. INTRODUCTION

Springs are significant ecological and cultural resources because they are essential for sustaining many ecosystems, serve as water sources for remote communities, are culturally or recreationally relevant in some regions, and could be the most sensitive indicators of climate change (Stevens et al., 2012). The scientific study of springs and their conservation worldwide has been hampered by the lack of a comprehensive classification system to quantify them (Alfaro and Wallace, 1994; in Springer and Stevens, 2008). Springs are occasionally the source of first-order water currents or lentic water bodies, and they are also part of a complex water system that involves both groundwater and surface water. Therefore, their protection and preservation are essential for the conservation of water resources in general.

In North America, where springs have been widely studied as they constitute the primary source of supply in some regions, the general definition of a spring is: "a place on the earth's surface where groundwater is discharged from the aquifer, creating a visible flow" (Kresic, 2010, p. 31). Meanwhile, in Colombia, springs are defined as “superficial discharge of groundwater that occurs through bedding planes or rock discontinuities such as fractures, cracks, or lithological changes, in areas where the topographic surface intersects the water table” (MADS, 2018, p. 13). Their classification, according to IDEAM et al. (2009), is limited to the mode of emergence at the surface (dripping or seepage), permanence (perennial, seasonal, or intermittent), and the nature of the conduits through which the water flows (karst, fracture, or contact). However, these classifications overlook the wide variety of geological settings across the country and the types of water discharging at the surface; therefore, springs deserve a more detailed characterization. In tropical countries like Colombia, with thick soils, significant rainfall, and abundant vegetation, the classic definitions of what a spring is may not fully describe the groundwater system, as they overlook other physicochemical processes that can create ambiguities in its definition and subsequent classification as protected zones.

In Colombia, springs are not well studied. To date, local or regional research on classification, systematic methodologies for comprehensive assessment, and the definition of emerging water types is unknown. The only approach to study them comes from the physicochemical characterizations that are a requirement to carry out infrastructure, mining, transportation, renewable and non-renewable energy projects before government entities (Regional Autonomous Corporations and the National Environmental License Authority – ANLA, by its Spanish acronym) in the framework of Environmental Impact Studies (EIA by its Spanish acronym). Therefore, many emerging bodies of water have been extensively referred to as springs, even though they do not meet the word's strict definition (Kirk,1919; Springer & Stevens, 2008; Stevens et al.,2012; IDEAM et al.,2009; Meinzer,1923a,b; Fetter,1994; Kresic, 2010), as some have a direct and immediate relationship with precipitation, flow through the vadose zone, but never reach the groundwater reserves.

In such a scenario, a clear methodology is needed to ensure unbiased classification of springs, especially in tropical countries and regions dominated by crystalline rocks. The answer might lie in the chemical properties of the water bodies (Ravikumar & Somashekar, 2017; Güler et al., 2002; Jalali & Jalali, 2016; Lourenço et al., 2010). Therefore, with this study, we propose a first approach to define the origin and type of water by using hydrochemical data from the Gramalote mining project (GCL, Gramalote Colombia Limited), located in the municipality of San Roque in the department of Antioquia, Colombia, where all water points have been named a priori as springs in the EIA.

The primary objective of this study was to elucidate the interactions between rainwater and the subsoil after infiltration and flow, using multivariate hydrochemical, physicochemical, and statistical analyses within the area’s hydrogeological context. The final goal was to classify the emerging waters (so-called springs) using a methodological categorization that would allow determining whether the water sampling points discharge from the aeration zone (vadose zone) or are part of the continuous discharge of a potential aquifer unit or saturated zone. Finally, it was possible to verify the initial hypothesis that not all points classified as springs can be called such; rather, some may have a unique relationship with rain or surface water and emerge at the surface due to slope or texture changes without necessarily being saturated-zone fluxes or aquifers.

2. GEOLOGICAL SETTING

The study area is located in the department of Antioquia, Colombia. It corresponds to the Gramalote mining project (GCL), located on the right bank of the Nus River (Figure 1), approximately 1 km south of the township of Providencia, a jurisdiction of the municipality of San Roque, 80 km northeast of the city of Medellin. The mining project's influence area, totaling 59 km2, is the same one used for the analyses in this study. The predominant geology is the Batolito Antoqueño, composed mainly of plutonic igneous rocks, specifically medium- to coarse-textured tonalites (Integral S.A., 2015). Within the unit, textural and compositional variations include quartz diorites, granodiorites, diorites, gabbros, dacites, and, to a lesser extent, aplite. Alluvial deposits are

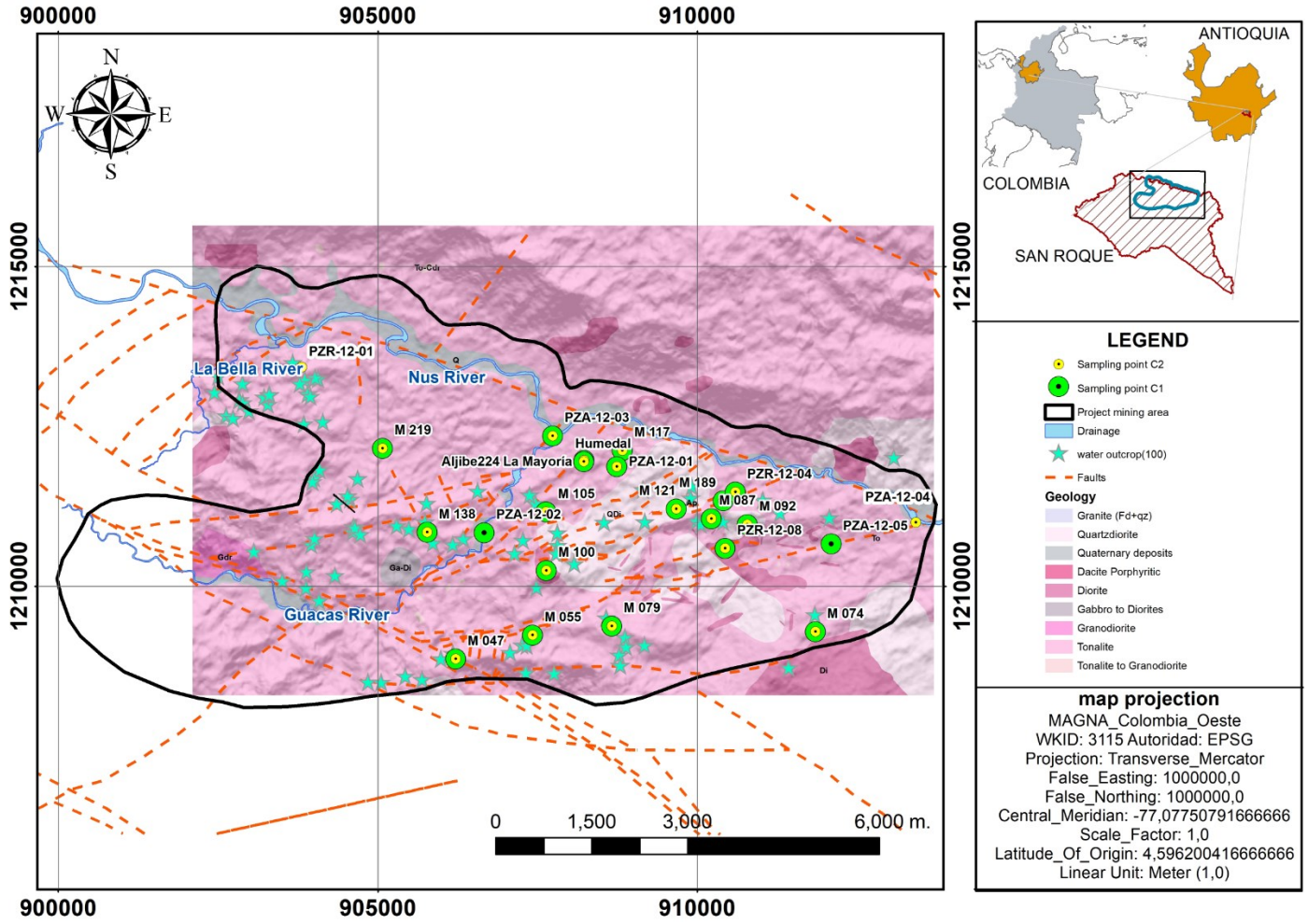

Figure 1. Location of the study area, surface geology, and existing water sampling points in the study area. Own elaboration, based on Integral S.A.

also associated with the Nus River and the Guacas Creek. Thin slope deposits also rest on the saprolite, which cannot be mapped due to the scale and extent of Figure 1.

Based on observations of drainage patterns, field surveys, photointerpretation results, and geomorphological features, a structural model was developed, highlighting the following structural trend: N45°W to N60°W, corresponding to the Nus River fault system, which controls several segments of major streams, including Guacas Creek. N45°E to N60°E, which controls the course of the Guacas creek before its confluence with the Nus River, and N–S ±10° and E–W ±10°. Additionally, no direct relationship was identified between joint density and hydraulic significance. Joint sets with high fracture density generally consist of closed or mineral-filled fractures (Integral S.A., 2015).

The annual average precipitation ranges from 2,000 to 4,000 mm, being higher towards the municipality of San Roque (southwest) and lower towards San José del Nus (northeast) (Integral S.A., 2015). However, the seasons from April to June and August to November are generally the wettest of the year, and recharge rates range from 7 to 22 l/s/km², or approximately 10 to 30% of annual precipitation (Golder Associates, 2014). The mean monthly temperature and evaporation at the El Nus Experimental Farm station are 26.3°C and 108 mm, respectively (Integral S.A., 2015). The topography consists of weathered hills with moderate to steep slopes and dense vegetation, with elevations ranging from 800 m.a.s.l. to just over 1300 m.a.s.l. (Golder Associates, 2014).

The surface distribution of the hydrogeological units shows no variation due to the predominance of the Antioquian Batholith's residual soil layer. That is why the defined hydrogeological units for the mining project, as described by Golder Associates (2014), outlined below, indicate that variations within these units occur at depth.

- HGU1 – Conformed by alluvial deposits present at the bottom of the valleys (more extensive in the Nus River valley), and by slope deposits partially covering the batholith.
- HGU2 – Residual soils as a thin layer over the entire area.
- HGU3 – Extremely weathered saprolite, a product of the Antioquia Batholith's weathering, where all the clay-forming minerals have been wholly weathered.
- HGU4 – Sandy saprolite from a mid-stage weathering process, in which the parent rock's crystal structure has broken down, but the clay-forming minerals show partial or minimal decomposition.
- HGU5/6 – Transition zone saprolite, product of an early weathering stage in which oxidation occurs, especially on the fracture faces, but with high rock resistance. Fractured rock is also included in this horizon and is likely to have hydraulic properties similar to the transition zone.
- HGU7 – Rocky basement, almost intact.

3. DATA AND METHOD

3.1.Monitored data and parameters. This research used secondary data collected during the Gramalote mining project's hydrogeological baseline study, and Gramalote Colombia Limited generously provided the dataset. The information from the Gramalote project (hereafter referred to as GCL) included an inventory of water sampling points, all of which had been classified as springs. The data came from four (4) campaigns carried out in 2011 (September to November), 2012-I (August to October), 2012-II (November to December), and 2019-2020 (December to July), in which 223, 250, 239, and 259 water sampling points (presumed springs) were inventoried, respectively.

Additionally, two (2) hydrochemical monitoring campaigns were conducted in 2012. The first campaign, in which 24 samples were collected, was conducted from March to June, during the first wet period of the year. During the second campaign, 22 samples were collected in October, during the transition period from wet to dry season in this region of Colombia. From each campaign, 21 samples met the acceptable ionic balance error criteria and were selected for further analysis. These 21 samples were from the so-called springs (13), the piezometers (6), and surface water (2).

From now on, the four (4) water sampling campaigns will be referred to as C1, C2, C3, and C4, while the two (2) hydrochemical campaigns will be named Campaign 1-HQ and Campaign 2-HQ or simply C1-HQ and C2-HQ.

Fifity-eight (58) hydrochemical variables were analyzed in the laboratory (major ions, minor ions, trace elements), and 12 variables were selected for multivariate statistical analyses and hydrogeochemical classification diagrams: electrical conductivity (EC), dissolved oxygen (DO), pH, Ca_2^+, Mg_2^+, Na^+, K^+, HCO_3, Cl^-, SO_4^{2-}, SiO_2, and Fe. The units for the concentration of major ions were mg/L, and for EC were µS/cm. These variables were selected because they best characterize the area's water type based on the outcropping geological units and, according to Güler and Thyne (2004), generally help accurately identify almost all environments

.

3.2.Database editing - Quality data evaluation. The water sampling points inventory data for all campaigns were organized and filtered to include only the persistently flowing points during the information-gathering period. If a sampling point dried up in at least one monitoring campaign, it was excluded from the analyses. The hydrochemical monitoring database was found to have censored data (some elements are reported as "less than"). For multivariate analyses, it is necessary to report a numerical value in each cell where this situation occurs. Therefore, a value of 0.55 times the lower detection limit was used in this study, following the recommendations of Van Trump and Miesch (1977), as cited in Güler et al. (2002).

The laboratory's hydrochemical data were verified as usable based on ionic balance (Freeze and Cherry, 1979). Although Hounslow (1995) and the Colombian Technical Guide GTC 30 (ICONTEC, 2014) indicate that only those samples with an analytical error less than or equal to 10% should be used, Custodio and Llamas (1975) suggest that the acceptable ionic balance error ranges depend on the electrical conductivity value, since the lower the electrical conductivity, the greater the acceptable error in the ionic balance; we decided to use this last criteria.

Finally, the geology, hydrogeological context, spatial distribution, and elevation were reviewed in the database for each water sampling point to understand the characteristics of these emerging waters, with a focus on the choice of hydrogeochemical diagramming and multivariate statistics at each point.

3.3.Descriptive statistics. Using the filtered databases and hydrochemical monitoring data from the inventory campaigns of the water sampling points, basic descriptive statistics (mean, standard deviation, and data asymmetry) were calculated to define the transformations to be employed in data preprocessing and multivariate statistical analyses. A preliminary data exploration was performed using histograms, box plots, and bivariate graphs for some parameters. Finally, using the filtered database of persistently flowing sampling points, spatial distribution maps of EC were generated for 100 springs across the four campaigns.

3.4.Data transformation and standardization. High positive asymmetry coefficients of hydrochemical variables, which did not follow a normal or close to normal distribution, were logarithmically transformed. For DO, Na^+, and SiO_2, a non-linear transformation was used (squared), as they are negative asymmetry parameters; this transformation compresses the scale for small values and expands it for large values (Marín, 2021). Afterward, all parameters were standardized to ensure that each variable was equally weighted, allowing for comparison across different units, as each variable carried the same weight in the statistical analyses. The standardization is needed in hierarchical cluster analyses, where the Euclidean distance is estimated, because if the variables do not have the same weight, this distance would be influenced by the variable with the highest magnitude or the one with a different measurement unit (Güler et al., 2002; Malagón et al., 2021).

Although electrical conductivity (EC) primarily reflects the major ions, tests were performed with and without EC in the Principal Component Analysis (PCA) and Hierarchical Cluster Analysis (HCA). Because the samples continued to group similarly with and without this parameter, it was decided to retain it, given the limited number of variables. Additionally, in other studies, EC has been used to analyze hydrochemical data using multivariate statistics (Ragno et al., 2007; Pazand and Javanshir, 2016; Ravikumar and Somashekar, 2017; Chen et al., 2018; Mostaza-Colado et al., 2018; Malagón et al., 2021).

Before selecting the optimal data treatment approach (in this case, transformation followed by standardization), multiple multivariate statistical analyses were conducted using the hydrochemical dataset. The analyses were first performed with raw data, then with standardized data only, then with normalized and standardized data, and finally, the chosen data were transformed and standardized, as described in the previous section. This last combination produced the most consistent results, in accordance with the hydrogeological understanding of the study area. Moreover, according to Cloutier et al. (2008), in multivariate cluster analysis, it is very common to apply variable transformation followed by standardization. There were no parameters without data; for Cl^- and $SO4^{2-}$, most reported values were censored by the method, which is why these parameters were removed from the EMV.

3.5.Multivariate statistical methods

3.5.1.Principal Component Analysis (PCA). PCA is a multivariate technique that explains the variance of a large set of correlated variables (measured physical parameters, anions, and cations) by reducing them to a smaller number of components, known as principal components (PCs). Most of the total variance of the hydrochemical variables can be explained by a smaller number of new, uncorrelated variables; therefore, the dimensionality of the data is reduced (Swan and Sandilands, 1995; Güler et al., 2002; Ragno et al., 2007; Lourenço et al., 2010). The first component accounts for most of the variation in the initial data, and subsequent components explain a smaller proportion of that variation (Lourenço et al., 2010). The components selected for this study were those with an eigenvalue greater than one (1), as they explain the majority of the variance (Malagón et al., 2021).

Principal Component (PC) loadings are the eigenvectors derived from a covariance or correlation matrix, which contain information about all variables combined into a single number. The variables with the highest positive and negative loads make the greatest contribution to the data set (Lourenço et al., 2010; Ravikumar and Somashekar, 2017); therefore, the loads were analyzed to provide a greater understanding of the processes responsible for the similarities in the variables. The software package used for this analysis was Minitab Release 14® (Minitab Inc., 2021).

3.5.2.Hierarchical Cluster Analysis (HCA). A hierarchical configuration groups elements in a tree-like structure, where the lowest levels are clustered within higher-level groups; this type of graph is known as a dendrogram (Davis, 1986). This method involves classifying water samples by forming clusters based on data similarity, using predefined variables that explain the technical reasons for these groupings. One of the most intuitive distances used in hydrochemistry is the Euclidean distance, employed in this study, because it produces more distinctive clusters (Güler et al., 2002).

A set of objects grouped numerically, similar to the previous one, forms a cluster of points in a multivariate space, and several algorithms are available to split them (Swan and Sandilands, 1995). In this study, the applied algorithm was Ward's linkage, which joins the observations (water samples) seeking to minimize the variance within each cluster. Subsequently, the combination that gives the smallest sum of squares within each cluster is chosen. This procedure creates homogeneous clusters with similar sizes (De la Fuente, 2011).

As Güler et al. (2002) and Cloutier et al. (2008) mention, the number of clusters in the HCA is defined by moving the position of the phenon line up or down the dendrogram. This evaluation is subjective, which makes the HCA a semi-objective method. In this study, the phenon line has been defined at Euclidean distances of 9 (C1-HQ) to 9.6 (C2-HQ), considering that the resulting groups have different chemistries and that the previously described water types (groundwater or superficial) are also

related to this grouping. The software package was Minitab Release 14 (Minitab Inc., 2021).

3.5.3.Factor Analysis (FA). The factor analysis further reduces the contribution of the less significant variables obtained in the PCA. By rotating the PCA-defined axes, a new set of variables known as the estimated varifactors (VF) is created. This study used the Varimax rotation after determining the principal components (PC) of the hydrochemical variables. The Varimax rotation distributes PC loadings, minimizing the number of large and small loadings to maximize their dispersion (Richman, 1986; in Singh et al., 2004).

3.5.4.Hydrochemical characterization.For each hydrochemical monitoring campaign that contains the hydrochemical variables, the water type and its relationship with different dissolved ionic species were evaluated to reveal the major ions' origins, the main hydrogeochemical processes, such as ion exchange or silicate alteration, and the possible origin of each emerging water point through the controlling mechanisms of water chemistry (Ravikumar and Somashekar, 2017).

For the hydrochemical facies classification, the Piper and Stiff diagrams were used to determine the degree of mineralization at each point. Stiff diagrams were created to represent the average chemistry of each cluster. The free software Diagrammes v6.76 (Simler, 2021) was used to construct both diagrams. The Gibbs diagram was used to identify the originating processes of water chemistry (rainfall, evaporation, water-rock interactions) by plotting TDS vs. Na^+, K^+, and Ca^{2+} cations (Gibbs, 1970). Although the Gibbs diagram was initially constructed for surface water and is sometimes considered inappropriate for groundwater analysis, it has been used in numerous hydrogeological studies (Marandi and Shand, 2018). Considering this, it was used in this study, as it was not the only tool utilized to analyze the data. Finally, the sampling points from both campaigns were spatially plotted in ArcGIS V10.2 (Redlands, C.E.S.R.I., 2011) to associate the hydrochemistry with the lithology and elevation.

3.6.Physicochemical Comparison: Springs vs. Rainwater. Correlation analyses were performed using a series of electrical conductivity measurements for three rainwater collectors and eight presumed springs. These data were recorded over one hydrological year during the GCL isotopic sampling campaign (2020–2021). The objective of this analysis was to identify water points whose electrical conductivity values were similar to those of rainwater. This methodological step allowed the classification of water points based on their physicochemical characteristics.

4. RESULTS

4.1.Monitored data and parameters

4.1.1.Water sampling points database (presumed springs)

From the inventory of sampling points for the four campaigns, which contained a total of 971 sampling points, the ones with missing data (dry points) were omitted. A database containing 100 sampling points per campaign was obtained, yielded a total of 400 (Table 1). For the first three campaigns, the CE showed little variation in the mean and median, though a slight upward trend over time is noticeable. For campaign 4, an increase of almost 50% in this variable is evident compared to previous campaigns.

Figure 2 shows that, across the four (4) water spring inventory campaigns, the EC at most of the sampling points was less than 100 µS/cm, which is low mineralization according to Rodier (1981) for the emerging waters at these sampling points. Campaigns C1 and C4 had the highest number of "outliers", as indicated by the wider ranges of EC values (Figure 2)..

Table 1. Average values of the in situ physicochemical parameters for the four inventory campaigns.

Campaign/Period	Hydrological regime	Average rainfall (m)*	Discharge rate (l/s)	Temperature (ºC)	pH	EC (µS/cm)	TDS (mg/l)	DO (mg/l)	Salinity (%)
C1: September-november (2011)	Wet ("La Niña)"	0.4328	0.24	22.20	6.8	8.6-187.0	59.1	4.9	0.05
C2: August-octubre (2012)	Wet	0.4157	0.23	23.48	7.1	11.1-194.4	50.1	6.6	0.05
C3: November-December (2012)	Dry	0.1585	0.24	23.48	6.9	35.7-259.0	50.7	6.1	0.05
C4: December - July (2019-2020)	Dry ("El Niño" – Normal)	0.2518	ND	23.24	7.1	42.4-327.0	73.6	6.3	0.08

*Average monthly rainfall of the period in which the campaign was carried out. ND: No data

The outliers detected in C1 and C2 were not consistent across the subsequent campaigns. Such deviations may be attributed either to human error or to measurement inaccuracies associated with the multiparameter device used during data collection

Generally, electrical conductivity shows an inverse linear relationship with elevation, where the higher the elevation, the lower the EC, and vice versa (Toro, 2020). On the other hand, dissolved oxygen is directly related to elevation, as it has higher concentrations in recently infiltrated water or rainwater (in topographically higher areas). Hence, a low DO concentration indicates that the water has had some transit time through underground medium and discharge zones in lower elevations (Mazor, 2003).

For the four campaigns, the relationship between elevation and electrical conductivity is inverse (Figure 3A). For EC in campaigns C3 and C4, and for DO in campaigns C2 through C4, data transformations were applied before ANOVA to meet its assumptions. When applying an ANOVA between both parameters, a statistically significant association was obtained, with 95% reliability between the two variables (Table 2). However, the estimated correlation coefficient was very low (0.3–0.4), suggesting that ECs at the same elevation can vary widely.

Hydrochemical database. From the total of 24 sampling points in the database, 21 that complied with the acceptable ionic balance error were selected for each campaign. Table 4 and Table 5 present the data for the two campaigns conducted in 2012, the C1-HQ campaign in the March-April wet season and the C2-HQ campaign in the October-December transition (to dry) season (Figure 1). The average monthly rainfall for each sampling campaign was 573 mm for C1-HQ and 268 mm for C-HQ (IDEAM, 2021).For both campaigns SO_4^{2-}y Cl^- were reported by the laboratory as censored values, meaning they were below the laboratory's method detection limit. These two parameters were excluded from the multivariate analysis.

For dissolved oxygen (DO), there was also no direct relationship in most of the campaigns, as expected (Figure 3B). Likewise, the correlation for each regression was very low (0.1–0.2), despite ANOVA indicating a statistically significant association at a 95% confidence level (Table 3).

In the study area, deeper groundwater with longer residence time generally exhibits lower pH values (as indicated by piezometers). This acidity is commonly associated with sulfide minerals formed during auriferous mineralization

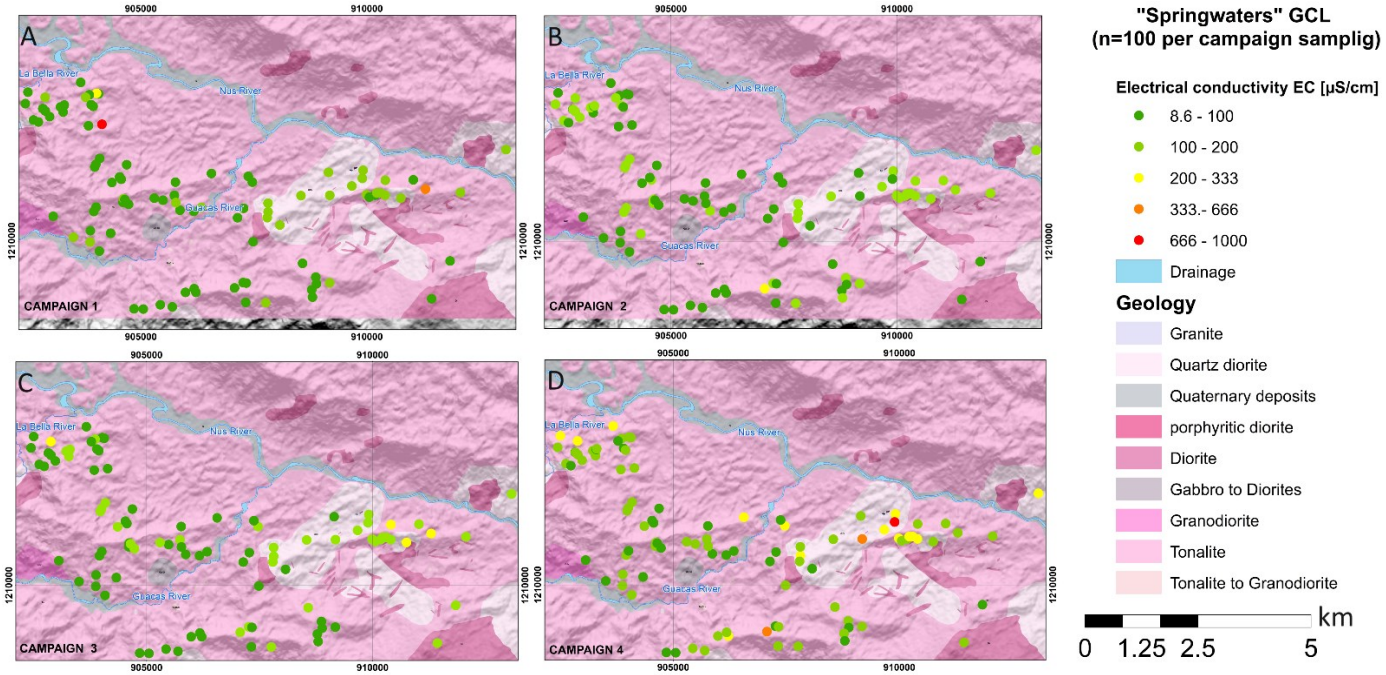

Figure 2. Map of the four campaigns (100 springs) with the EC's spatial distribution: A. Campaign C1, B. Campaign C2, C. Campaign C3, D. Campaign C4. EC ranges in µS/cm according to Rodier (1981): Low [<333], Medium [333-666], Moderate [666-1000], and High [>1000].

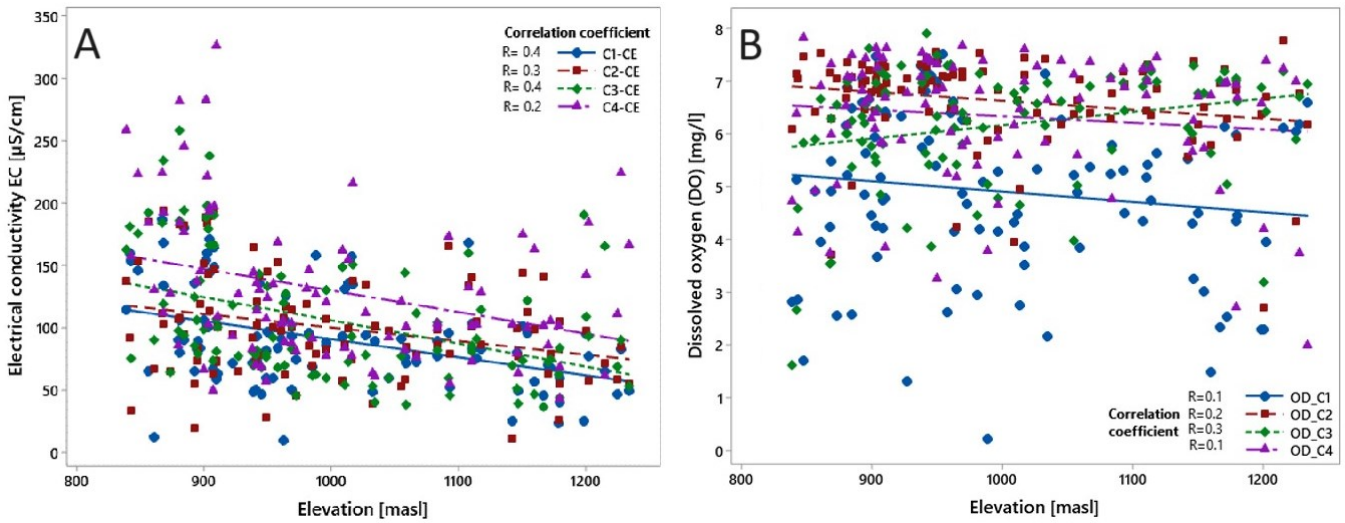

Figure 3. Linear regressions between the electrical conductivity (A) and the dissolved oxygen (B) with the height (elevation in m.a.s.l.).

Table 2. ANOVA results in the EC parameter for the four (4) inventory campaigns.

Campaigns		Degrees of freedom	Sum of squares	Mean Squares	F-Test	Critical F values
C1	Regression	1	26078.6	26078.6	19.4	0.0
	Residuals	95	127612.9	1343.3		
	Total	96	153691.4			
C2	Regression	1	14366.1	14366.1	9.0	0.0
	Residuals	97	154152.4	1589.2		
	Total	98	168518.5			
C3	Regression	1	238343.7	238343.7	22.6	0.0
	Residuals	97	1021054.3	10526.3		
	Total	98	1259398.0			
C4	Regression	1	0.3	0.3	10.4	0.0
	Residuals	90	2.9	0.0		
	Total	91	3.2			

Table 3. ANOVA results in the DO parameter for the four (4) inventory campaigns

Campaigns		Degrees of freedom	Sum of squares	Mean Squares	F-Test	Critical F values
C1	Regression	1	4.8	4.8	1.9	0.2
	Residuals	98	251.7	2.6		
	Total	99	256.6			
C2	Regression	1	0.1	0.1	5.5	0.0
	Residuals	98	1.9	0.0		
	Total	99	2.0			
C3	Regression	1	0.2	0.2	5.8	0.0
	Residuals	98	2.6	0.0		
	Total	99	2.8			
C4	Regression	1	0.0	0.0	1.1	0.3
	Residuals	98	3.5	0.0		
	Total	99	3.5			

Table 4. Hydrochemical monitoring points Campaign 1-HQ-2012-I, March-April (wet season).

Point name	Type	Elev.	DO	pH	EC	Ca_2^+	Mg_2^+	Na^+	K^+	HCO_3^-	Cl^-	SO_4^{2-}	Fe	SiO_2	TDS
M 100	Spring	1,098	4.2	6.8	96	10.1	2.6	8.0	0.8	42.4	3.5	2.75*	0.5	42.4	55
M 105	Spring	899	5.9	6.9	68	9.0	2.3	6.1	1.1	35.7	1.1*	2.75*	0.2	33.8	40
M 117	Spring	849	4.6	6.3	102	16.2	1.6	6.9	1.1	53.5	1.1*	2.75*	0.1	39.6	59
M 121	Spring	846	4.7	6.7	181	20.2	5.2	11.6	1.8	85.9	1.1*	2.75*	0.2	43.7	94
M 138	Spring	995	4.8	7.0	64	5.0	1.3	8.1	1.3	32.6	1.1*	2.75*	0.2	40.0	48
M 189	Spring	855	4.1	6.6	199	24.6	6.3	10.4	2.8	102.8	6.5	2.75*	0.6	52.4	112
M 219	Spring	899	3.9	6.0	58	5.0	1.3	7.7	1.0	21.7	1.1*	2.75*	1.1	30.7	35
M 047	Spring	1,227	4.9	5.9	36	11.2	2.9	3.1	1.3	43.1	1.1*	2.75*	0.1	25.0	49
M 055	Spring	1,149	4.9	6.1	122	8.2	3.0	9.3	0.8	42.0	7.0	2.75*	0.3	33.2	67
M 074	Spring	1,113	3.9	6.6	64	6.7	1.7	1.6	0.3	19.2	1.1*	2.75*	0.5	5.7	20
M 079	Spring	1,149	3.0	6.0	77	10.6	2.7	7.3	1.0	32.0	1.1*	2.75*	0.3	33.1	42
M 087	Spring	903	3.2	6.7	79	12.9	3.3	9.1	1.4	53.1	1.1*	2.75*	0.9	50.2	57
M 092	Spring	908	5.2	7.4	132	18.5	4.8	8.0	1.5	69.8	1.1*	2.8	0.4	48.5	76
Aljibe224	Surface water	850	1.6	6.6	59	4.8	1.7	5.8	1.0	26.3	1.1*	2.75*	2.1	21.0	35
PZA-12-01	Piezometer	849	2.3	5.9	90	6.4	1.0	11.2	1.1	47.9	1.1*	2.75*	5.5	52.6	49
PZA-12-02	Piezometer	846	1.1	5.6	79	11.6	1.6	5.2	2.0	40.3	1.1*	7.8	3.5	41.5	46
PZA-12-03	Piezometer	842	2.9	5.6	311	3.6	1.6	10.5	1.1	37.3	2.5	2.75*	6.1	35.0	42
PZA-12-05	Piezometer	850	2.7	5.8	95	6.4	0.7	9.8	1.1	37.3	1.1*	2.75*	5.9	33.9	40
PZR-12-08	Piezometer	955	2.2	5.8	160	10.4	0.5	7.5	2.3	29.2	2.5	2.75*	21.3	20.1	45
PZR-12-04	Piezometer	849	2.8	6.6	93	24.8	14.4	10.6	6.2	215.4	1.1*	22.6	4.3	44.9	240
Humedal La Mayoría	Surface water	835	2.3	6.3	58	6.2	1.6	5.9	0.8	19.4	1.1*	2.8	0.9	22.1	19

Elev.: elevation in m.a.s.l. (meters above sea level). DO: dissolved oxygen. EC: electrical conductivity. SDT: Total Dissolved Solids. Majority ion units, TDS and DO = (mg/l); pH = (pH Units); EC = (µS/cm). * Censured values by the laboratory interpreted as detection limit concentrations and multiplied by a factor of 0.55 for correction. The classification of springs is defined by the EIA, not by this study.

Of the 21 points selected, 13 were classified as springs in the study from which the data were extracted (Integral, 2015); six (6) were alluvial and rock piezometers, and two points called "Aljibe 224" and "Humedal La Mayoría" are influenced by surface water since "Humedal La Mayoría" is sustained only by a surface current and provides the water extracted in "Aljibe 224". These results are based on field observations.

It is highlighted that, for C2-HQ, the points named PZA-12-02 and PZA-12-05, which were sampled in C1-HQ, did not exist because they were dry. Therefore, they were replaced by PZR-12-04 and PZA-12-04. Although this work focuses on the springwaters, due to the limited amount of data available for the area, information from surface water and other groundwater sampling points was included to examine how the presumed springs clustered with different water types.

4.2.Hydrogeological context. Geologically, most of the so-called springs in the hydrochemical database emerge in the saprolite of the different geochemical facies of the Antioquian batholith. In contrast, only three (3) sampling points emerge from fractures of this same lithology. The alluvial piezometers are very shallow, with depths not exceeding 9 meters, while the rock piezometers have depths between 42 and 75 meters. Hydrogeologically, the saprolite is a transitional unit for water, lacking exploitable hydrogeological properties with aquifer potential.

Groundwater flow in the study area occurs primarily in the sandy saprolite and fractured rock horizons, with limited flow in the granodiorite, as indicated by the piezometer instrumentation (Golder Associates, 2014; Integral, 2015). The different hydrogeological units do not form an exploitable aquifer, even though there may be water storage and transit at the sandy saprolite (HGU-4) or through fractures (HGU-5 and 6), in concordance with the existing conceptual model's findings (Golder Associates, 2014; Integral, 2015).

In the monitored springs in the four (4) inventory campaigns, it is observed that these points are spread throughout the study area at different elevations. However, most of them (51%) geologically emerge at slope deposits overlying the batholith's residual or saprolite. The remaining 46% emerge at the interface between the residual soil and the saprolite or transition zone, and 3% directly on the rock, as evidenced by the EIA conducted by Integral S.A. (2015).

Table 5. Hydrochemical monitoring points Campaign 2-HQ 2012-II, October-December (wet-dry transition season).

Point name	Type	Elev.	DO	pH	EC	Ca_2^+	Mg_2^+	Na^+	K^+	HCO_3^-	Cl^-	SO_4^{2-}	Fe	SiO_2	TDS
M 100	Spring	1,098	5.4	7.5	94	7.8	2.9	6.8	1.6	51.0	0.0	2.75*	0.6	17.2	53
M 105	Spring	899	6.7	6.9	160	13.8	0.0	8.5	2.6	73.6	1.1*	2.75*	0.2	31.9	88
M 117	Spring	849	3.9	6.3	19	6.6	4.6	6.1	1.6	55.4	1.1*	2.75*	0.2	39.5	57
M 121	Spring	846	6.4	7.5	178	13.1	5.6	16.0	3.2	98.1	1.1*	2.75*	0.1	50.9	104
M 138	Spring	995	6.5	6.2	7	4.2	1.3	8.9	2.4	33.9	1.1*	2.75*	1.1	17.5	36
M 189	Spring	855	3.0	6.7	191	17.4	8.2	10.5	3.3	106.2	1.1*	2.75*	0.2	21.8	110
M 219	Spring	899	6.4	6.9	46	3.2	1.0	5.4	1.5	23.3	1.1*	2.75*	0.6	27.1	250
M 047	Spring	1,227	5.4	7.5	94	7.8	2.9	6.8	1.6	51.0	1.1*	2.75*	0.6	17.2	53
M 055	Spring	1,149	5.5	6.5	104	9.9	2.9	9.4	0.6	44.4	5.0	2.75*	0.3	15.5	63
M 074	Spring	1,113	6.5	6.9	43	4.2	2.0	3.2	0.6	21.5	1.1*	2.75*	0.7	5.6	35
M 079	Spring	1,149	3.7	6.5	62	6.2	2.2	5.9	1.1	37	1.1*	2.75*	0.6	14.9	40
M 087	Spring	903	6.0	6.3	63	4.1	1.8	2.6	1.0	19.4	1.1*	2.75*	0.5	30.4	35
M 092	Spring	908	6.5	6.0	108	9.2	4.0	6.6	2.1	57.6	1.1*	2.75*	0.3	17.3	61
Aljibe224	Surface water	850	2.1	6.5	78	7.8	1.1	9.7	1.1	42.3	2.0	5.0	4.2	13.1	44
PZA-12-01	Piezometer	849	1.4	6.8	95	4.5	1.4	15.0	1.9	43.5	1.1*	2.75*	2.8	44.6	45
PZA-12-02	Piezometer	846	2.0	6.5	120	6.1	7.4	15.0	2.8	40.8	12.5	2.75*	8.2	29.5	45
PZA-12-03	Piezometer	842	1.3	6.8	311	25.6	15.2	9.5	1.3	132.1	1.1*	2.75*	9.7	59.3	160
PZA-12-05	Piezometer	850	2.0	6.1	85	5.3	1.4	8.8	3.9	30.2	1.1*	2.75*	4.1	34.9	41
PZR-12-08	Piezometer	955	2.4	6.6	234	38.2	1.4	18.5	2.7	117	2.0	5.0	0.8	18.8	141
PZR-12-04	Piezometer	849	3.1	7.5	391	27.6	19.6	9.7	9.5	210.5	1.1*	13.9	1.4	28.0	228
Humedal La Mayoría	Surface water	835	2.0	6.6	50	3.4	1.0	8.4	0.6	27.8	1.1*	2.75*	3.7	11.7	36

Elev.: elevation in m.a.s.l. (meters above sea level). DO: dissolved oxygen. EC: electrical conductivity. SDT: Total Dissolved Solids. Majority ion units, TDS and DO = (mg/l); pH = (pH Units); EC = (µS/cm). * Censured values by the laboratory interpreted as detection limit concentrations and multiplied by a factor of 0.55 for correction. The classification of springs is defined by the EIA, not by this study.

4.3.Multivariate statistical methods - Hydrochemical Database

4.3.1.Principal Component Analysis (PCA) / Factor Analysis (FA). In this study, PCA/FA was applied to compare the composition patterns of the analyzed water samples. Table 6 presents the eigenvalues, the percentage of explained variance, and the accumulated eigenvalues of the PCA for both HQ campaigns.

In hydrochemical studies of natural waters, the literature shows that PC1 and PC2 typically explain only 40–55% of the total variance, especially in complex geological settings. Therefore, most multivariate analyses use 3 to 5 factors—sometimes up to 5 or 6—to account for 70–80% of the variance (Cloutier et al., 2008; Lourenço et al., 2010; Pazand and Javanshir, 2016; Ravikumar and Somashekar, 2017). For a more straightforward PCA interpretation, an FA (Factor Analysis) was applied. The four (4) factors that explained an acceptable level of variance in Table 6 (□70%) were retained, which, for descriptive purposes, would require explaining 80% of the variance (Minitab Inc., 2021). Table 7 presents the rotated load matrix, eigenvalues, and percentage of variance explained for both campaigns.

Based on Helena et al. (2000), Cloutier et al. (2008), Ravikumar et al. (2017), and Bodrud-Doza et al. (2016), a factor is considered valid when it explains more than 10% of the total variance, presents strong loadings (≥ 0.5), and has a consistent hydrogeochemical interpretation. The global interpretation of FA is typically accepted when the cumulative variance of the retained factors exceeds 60–70%, as in our study.

In the C1-HQ campaign, the first four factors accounted for 85% of the total variance in the matrix (Table 7). According to the observations projections, when plotting the first component (PC1) against the second component (PC2) and the respective factor loads (Figure 4 and Table 7), it is observed that the first axis explains almost 32% of the total variance, where the highest and most positive parameter loads are (0.5 to 0.9), such as HCO^3, SiO_2, Ca^{2+}, Mg^{2+}, K^+. Factor 2 accounts for about 22% of the total variance, with high positive loadings for SiO_2, EC, and Na^+. Factor 3 explains 20% of the variance, with the highest negative load on Fe and a positive load on DO. Factor 4 explains 11% of the variance and has a strong positive loading on pH.

In the C2-HQ campaign, the first five factors account for 69% of the total variance of the original matrix (Table 7). According to the observations, projections, and the respective factor loadings (Figure 5 and Table 7), the first axis explains 24% of the total variance. The parameters with the highest and most positive loads (0.8 and 0.9) are HCO^{3-}, Ca^{2+}, and CE.

Factor 2 explains about 17% of the total variance, with high loadings on HCO^{3-}, Na^{+}, and K^{+}. Factor 3 explains 16% of the variance, and the highest load is for OD (0.8) and Fe (-0.8). Factor 4 explains that 11% of the variance and has the highest load for pH (-0.96). The grouping of observations across the variables revealed three similar clusters in both campaigns, with cluster 3 comprising two presumed springs and the alluvial and rock piezometers (Table 8).

4.3.2.Hierarchical Cluster Analysis (HCA). For the two campaigns, a hierarchical cluster analysis was performed using Euclidean distance and Ward's linkage. A total of 12 variables from 21 samples per campaign were used, resulting in three clusters, as shown in the dendrograms (see Figure 10). The phenon line in both campaigns was defined based on the previous PCA results, which indicated three clusters that were consistent not only with the type of sampling point (e.g., surface water, piezometers, springs) but also with the distribution of major ions and field parameters such as pH, DO, and EC for each water type. Therefore, the phenon line was drawn to produce three clusters.

In campaign 1, cluster 1 groups the points classified as springs, with "Aljibe 224" and "Humedal La Mayoría" mainly related to surface water. Cluster 2, in both campaigns, grouped the piezometers with alluvial and rock. However, cluster 3 was the only one that, in both cases, included two presumed springs, M189 and M121, which showed higher concentrations of major ions and EC than the other similar sampling points and were grouped with water from alluvial and rock piezometers.

Table 6. Analysis of the covariance matrix's eigenvalues and eigenvectors for the two HQ campaigns.

	C1-HQ					**C2-HQ**				
Principal component	1	2	3	4	5	1	2	3	4	5
Eigenvalue	4.16	2.59	1.05	0.74	0.50	4.124	1.839	1.088	0.844	0.734
% of explained variance	42%	26%	11%	7%	5%	41%	18%	11%	8%	7%
Cumulative variance %	42%	68%	78%	85%	**90%**	41%	60%	71%	79%	**86%**

Table 7. Matrix of principal components with Varimax rotation and loads of the principal components rotated.

C1-HQ					**C2-HQ**				
Variable	**Factor 1**	**Factor 2**	**Factor 3**	**Factor 4**	**Variable**	**Factor 1**	**Factor 2**	**Factor 3**	**Factor 4**
DO	0.08	0.04	**0.93**	0.10	**DO**	-0.20	-0.25	**0.82**	0.10
pH	0.09	-0.08	0.25	**0.93**	**pH**	0.23	0.10	0.11	**0.96**
EC	0.10	**0.85**	-0.04	-0.22	**EC**	**0.73**	0.18	-0.19	0.29
Ca_2^+	**0.89**	0.09	0.23	0.02	**Ca_2^+**	**0.94**	0.33	0.03	0.05
Mg_2^+	**0.76**	0.11	0.31	0.31	**Mg_2^+**	0.19	0.34	-0.24	0.11
Na^+	0.26	**0.89**	-0.15	0.03	**Na^+**	0.37	**0.52**	-0.33	0.04
K^+	**0.82**	0.22	-0.34	-0.08	**K^+**	0.28	**0.67**	0.04	0.06
HCO_3^-	**0.88**	0.43	0.05	0.04	**HCO_3^-**	**0.77**	**0.60**	0.03	0.17
Fe	-0.08	0.22	**-0.90**	-0.22	**Fe**	-0.09	-0.03	**-0.83**	-0.03
SiO_2	**0.53**	**0.62**	0.03	0.22	**SiO_2**	0.10	0.57	-0.08	0.02
Variance	3.20	2.20	2.02	1.12	**Variance**	2.38	1.73	1.58	1.07
% Var	**32%**	**22%**	**20%**	**11%**	**% Var**	**24%**	**17%**	**16%**	**11%**
Cumulative	**32%**	**54%**	**74%**	**85%**	**Cumulative**	**24%**	**41%**	**57%**	**68%**

*Values in bold correspond to the parameters with the highest factor loadings contributing to the explained variance.

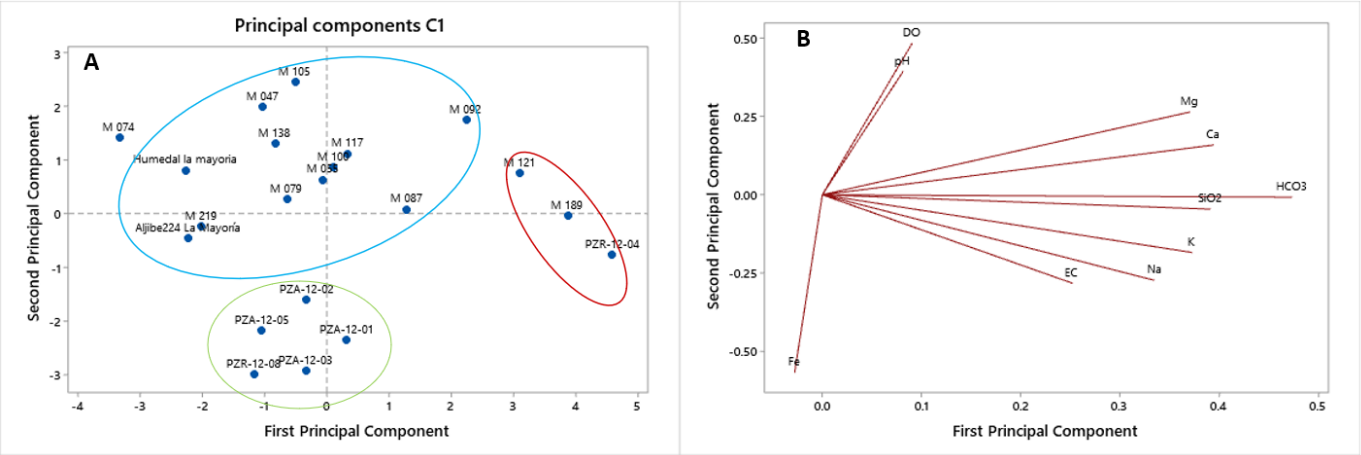

Figure 4. A) Principal Components C1-HQ observation points. B) Principal Components C1-HQ physicochemical parameters.

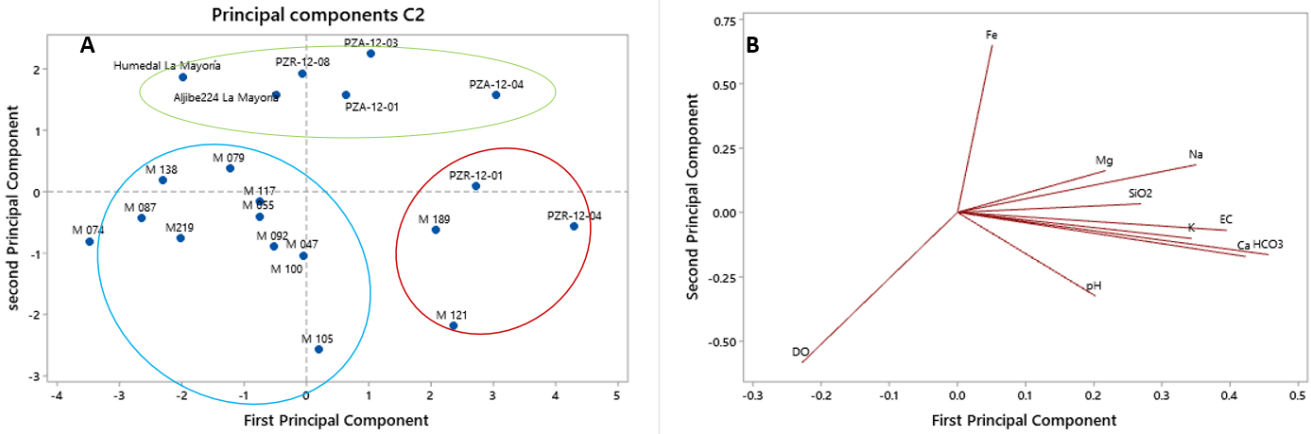

Figure 5. A) Principal Components C2-HQ observation points. B) Principal Components C2-HQ physicochemical parameters.

Table 8. Clusters in both campaigns and hydrochemical variables associated with each cluster.

Cluster	Samples	Associated variable
C1-HQ-2012-I, March-April		
Cluster 1	M 100, M105, M117, Humedal La Mayoría, M138, Aljibe224, M219, M047, M055, M074, M079, M087,M092	pH, DO
Cluster 2	PZA-12-01, PZA-12-02, PZA-12-03, PZA-12-05, PZR-12-08	Fe
Cluster 3	PZR-12-04, M189, M121	EC, K^+, Na^+, Ca^{2+}, Mg^{2+}, HCO_3^- y SiO_2.
C2-HQ 2012-II, October -December		
Cluster 1	M 100, M105, M117, M138, M092, M219, M047, M055, M074, M079, M087	DO, pH
Cluster 2	PZA-12-01, PZA-12-03, PZR-12-08,PZA-12-04, Humedal La Mayoría, Aljibe224,	Fe
Cluster 3	PZR-12-01, PZR-12-04, M121, M189	EC, K^+, Na^+, Ca^{2+}, Mg^{2+}, HCO_3^- y SiO_2.

4.4. Hydrochemical characterization

4.4.1.Water types. The Piper diagrams for both campaigns (Figure 6) show that most of the samples springs, piezometers, and "Aljibe 224") are Ca_2^{+}–HCO_3^{-} waters. Some samples had sodium as the dominant cation and were classified as Na+–HCO3- (purple circle in Figure 6).

The central hypothesis is that most of the points labeled as springs in the database are directly related to rainfall. Therefore, the Gibbs diagram was used to identify the processes driving water chemistry and to confirm this hypothesis. For campaign 1 (Figure 7), it was observed that springs, piezometers, "Humedal La Mayoría," and "Aljibe 224" were grouped in the field with a primary physicochemical process driven by rainfall. On the other hand, a rock piezometer (PZR-12-04) and two springs (M121 and M189) exhibited a predominance of water-rock interaction based on the amount of TDS and the K^{+}, Na^{+}, and Ca^{2+} cations. These last sampling points are part of cluster 3, previously identified in the multivariate analyses in the two HQ campaigns.

For campaign 2 (Figure 7), the points with a predominant water-rock interaction are rock and alluvial piezometers (PZA-12-04/PZR-12-01/ PZR-12-04), and the presumed M189, M121, and M219 springs, where predominates K^{+}, Ca^{2+}, Na^{+}, Mg^{2+}, HCO^{3-}, SiO_2, and Fe ions. Some of them are also part of the previously mentioned cluster 3, while the rest are in the rainfall field. The Gibbs diagram is used merely as a complementary hydrochemical tool to support the interpretation of cluster origins. Although the Gibbs approach is widely recognized for identifying the dominant geochemical processes controlling groundwater composition (Sun et al., 2021b; Yin et al., 2021; Zhao et al., 2022), it was not used in isolation to derive the final conclusions.

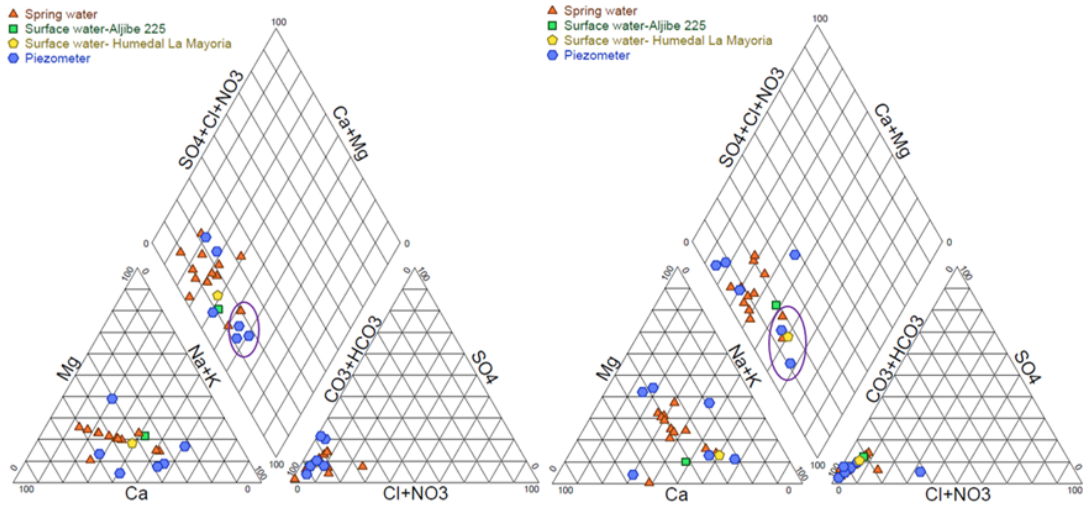

Figure 6. Piper diagrams. A) Campaign C1-HQ, B) Campaign C2-HQ.

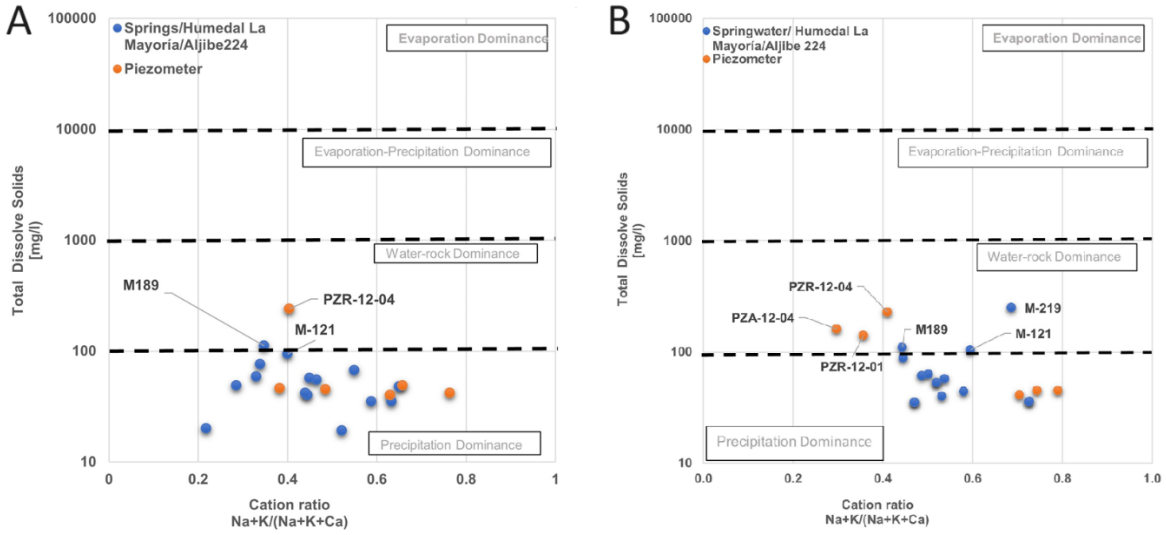

Figure 7. Gibbs diagrams. A. Campaign C1-HQ, B. Campaign C2-HQ.

4.4.2.Ionic relations. The water samples were plotted according to their corresponding cluster (Figure 8 and Figure 9). In Figure 8A, most of the samples were above the 1:1 line (e.g., M189-M121) and a few below (e.g., M92, M79, M74), reflecting the occurrence of either silicate alteration or CO2 hydrolysis in the vadose zone (Lakshmanan et al., 2003; Elango and Kannan, 2007; Kumar et al., 2009; Zhang et al., 2020). Due to the limited number of samples and the scarcity of available data, and while fully acknowledging the limitations associated with using censored data, we chose to include these values in the hydrochemical (HQ) analyses to maintain data representativeness.

In Figure 8B if the HCO3- content is greater than Na+, or the HCO^{3-}/ Na^{+} ratio is between 1:1 and 1.18: 0.82, it means there is a silicate alteration (Lakshmanan et al., 2003; Elango and Kannan, 2007; Zhang et al., 2020), but if they are not between these stoichiometric lines, it means that there is a cation exchange and most of the sampling points would be above-said lines.

In Figure 8C, the ($K^{++}Na^{+}$)/total cations index indicates that sampling points above the ($K^{++}Na^{+}$) = 0.5 TZ+ line would be associated with silicate weathering (Lakshmanan et al., 2003). However, most sampling points in C1-HQ are located on the ($K^{++}Na^{+}$) = 0.33 line, consistent with the Ca^{2+}/Na^{+} exchange process (Lakshmanan et al., 2003; Jalali, 2007). Finally, if the molar ratio of Figure 5D Na^{+}/Cl^{-} is greater than 1, it indicates silicate weathering or cation exchange (Zhang et al., 2020), which occurs for the C1-HQ samples. The same behavior observed for C1-HQ also occurs for C2-HQ; the graph is shown in figure 9

4.4.3.Hydrochemistry according to clusters. Average Stiff diagrams were plotted for the three clusters defined for each campaign. For campaigns C1-HQ and C2-HQ (Figure 10), the average Stiff diagrams showed similar behavior, where the water samples from clusters 1 and 2 are the least mineralized. However, after examining the content of the 12 measured variables, it was evident that cluster 2 had higher concentrations of Na^{+} and Fe, while DO and pH were lower than those of cluster 1; therefore, they are separated into two distinct groups.

Spatially, cluster 1 points (in both campaigns) are predominantly located in the upper part of the area, at elevations between 900 and 1,200 m.a.s.l. (Figure 10), although there are also some points towards the middle and lower sections. In addition, they are geologically associated with tonalite and quartz diorite saprolite; only two points are present in fractured rock. Cluster 2 is in the lower and middle sections of the area (elevations between 830 and 870 m.a.s.l.), associated mainly with alluvial deposits. Cluster 3 is in the lower section (830 to 870 m.a.s.l.), primarily emerging through the tonalite and quartz diorite fractured rock and, to a lesser extent, in saprolite or alluvial deposits.

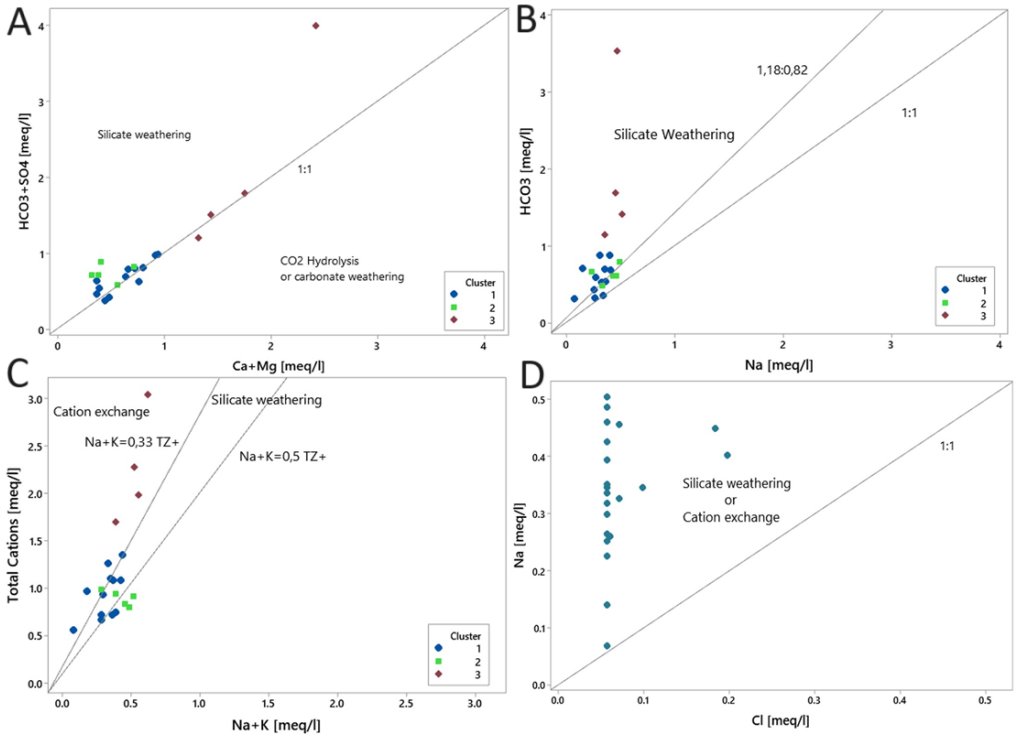

Figure 8. Ionic relations for C1-HQ. A. HCO3- + SO42+ vs Ca2++ Mg2+; B. HCO3- vs Na+; C. Total cations vs Na++ K+; D. Na+ vs Cl-.

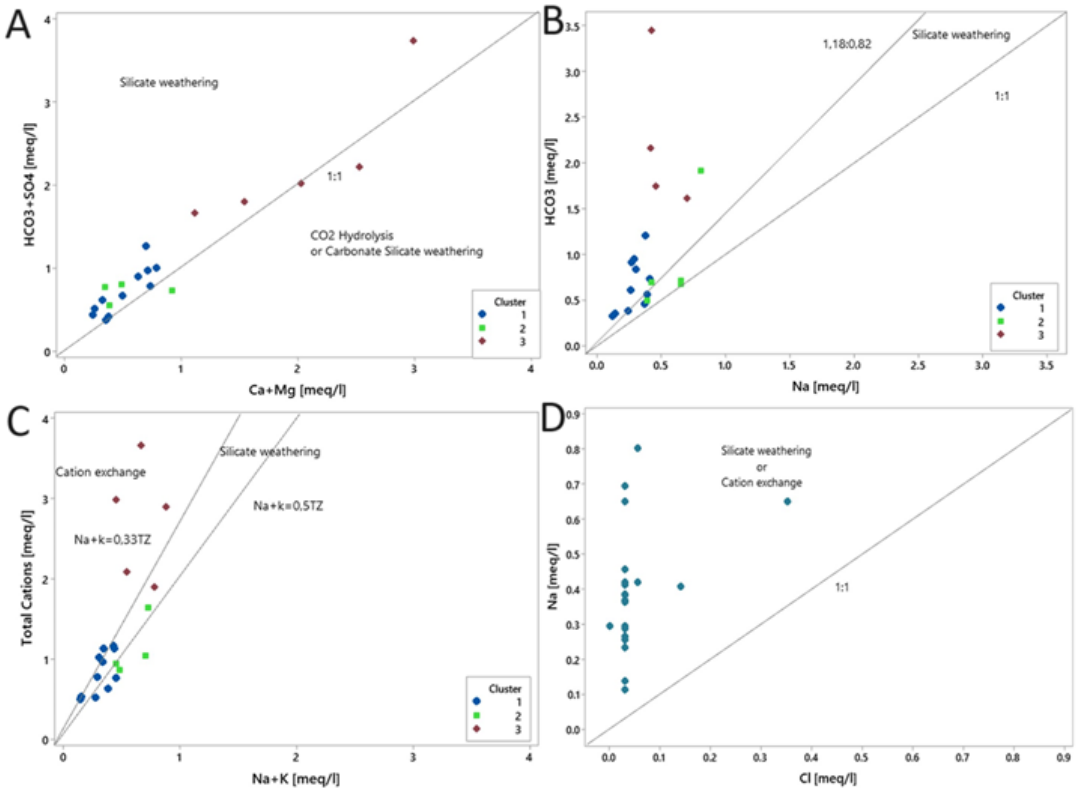

Figure 9. Ionic relations for C2-HQ. A. HCO3- + SO42+ vs Ca2++ Mg2+; B. HCO3- vs Na+; C. Total cations vs Na++ K+; D. Na+ vs Cl-.

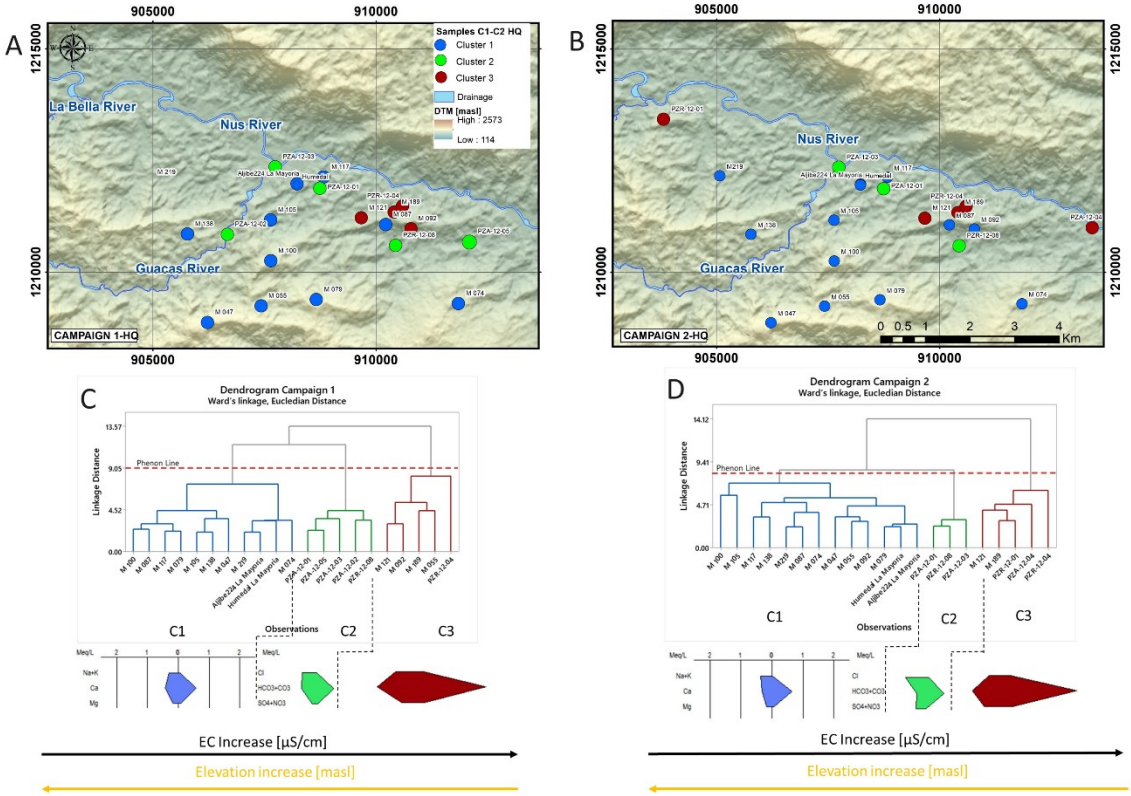

Figure 10. Maps with the Digital Terrain Model (DTM) in m.a.s.l. with both campaigns' clusters' locations: A) Campaign 1, B) Campaign 2. HCA campaigns C1-HQ (C) and C2-HQ (D). The dendrograms show the three main groups. Stiff diagrams represent the average concentration of major ions in milliequivalents per liter (meq/L).

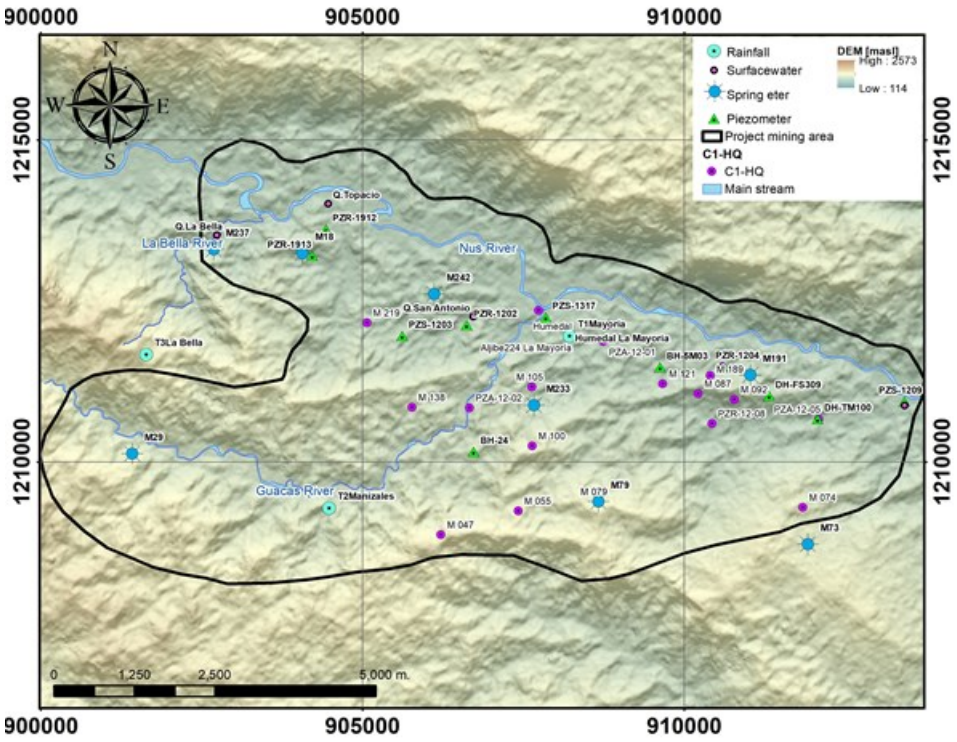

Figure 11. Spatial Distribution of EC Sampling Points for 2020–2021 and C1-HQ

4.5.Physicochemical Comparison: Springs vs. Rainwater

Analyses were carried out using EC data from eight (8) springs, seven (7) surface waters, eleven (11) piezometers, and three (3) rainwater collectors from the GCL project, referred to as T1 La Mayoría, T2 Manizales, and T3 La Bella (Figure 11). It is worth noting that these piezometers are not the same sampling points used in the hydrochemical campaigns. These measurements were recorded between January 2020 and March 2021

Table 9 presents the average in-situ physicochemical parameters for each water type measured in the GCL project (SHI SAS, 2021). The results show that the average parameter values at spring-type points are more similar to those of surface water and rainfall than to those of groundwater. As expected, rainwater has the lowest electrical conductivity of the water types (IDEAM, 2022).

Since electrical conductivity is the most conclusive of the in-situ parameters—because it reflects the concentration of ions dissolved in the water, where higher electrical conductivity indicates higher ion and dissolved solids content (Domenico & Schwartz, 1998)—the EC time series of the springs and rainfall in the study area were used to calculate the correlation coefficient between each spring and rainfall. It is worth noting that the rainfall collector T1 La Mayoría is located at the lowest elevation in the area (836 m.a.s.l.) (Figure 11). In contrast, collectors T2 and T3 are located at elevations of 1270 m and 1301 m.a.s.l., respectively.

Although collector T1 is geographically closer to springs M18, M233, M237, M191, and M2442, and collectors T2 and T3 are closer to springs M29, M73, and M79, correlations were calculated for all spring points against collectors T1 and T3 (Table 10-Figure 11), as these had the most complete datasets. This was done to assess whether springs located at lower elevations could be related to rainfall occurring at higher elevations. According to the correlation results (Table 10), springs M233 and M191 yielded positive correlation coefficients of 0.7 and 0.6, respectively, with T1. Meanwhile, springs M18, M191, and M73 showed similarly high correlations with T3 (0.6-0.7). Notably, M18 and M191 are located at lower elevations but still correlate well with rainfall measured at higher elevations.

This result shows a correspondence between the variability of electrical conductivity in rainfall and that observed in the springs. During the months when rainfall conductivity increases or decreases, the springs exhibit the same trend, even though EC values in spring water are slightly higher than those in rainwater. This behaviour is expected, as once rainfall infiltrates the soil, the electrical conductivity can increase due to the mobilization of fine particles and the hydrolysis of CO_2, which promotes bicarbonate release and enhances mineral weathering in the vadose zone.

Table 10. Pearson's Correlation Matrix between T1, T3, and Water Sampling Sites

	M233	***M18***	***M237***	***M242***	***M191***	***M29***	***M79***	***M73***
Correlation T1	0.7	0.1	-0.1	0.1	0.6	-0.2	0.0	-0.3
	M233	**M18**	**M237**	**M242**	**M191**	**M29**	**M79**	**M73**
Correlation T3	0.3	0.7	-0.1	0.0	0.6	0.4	-0.1	0.7

5. DISCUSSION

This research aimed to investigate and identify the hydrochemical and hydrogeological characteristics of the presumed springs in the study area, thereby elucidating their origin and confirming their classification. The results obtained from different sources, types of information, and methodological steps made it possible to conclude that not all the so-called springs could be strictly classified as such. Instead, some of these have a unique relationship with rainwater. These water sampling points have been indiscriminately labeled as springs (in the EIA data source) even though they do not originate from the saturated zone.

In this study, on-site physicochemical information and laboratory analysis of major ions were available. The on-site physicochemical parameters for the four (4) sampling-point inventory campaigns (Table 1) showed that these points correspond to oxygenated and freshwater conditions, as the DO levels are typical of recently infiltrated water, generally greater than 5 mg/L and similar to rainwater. The EC and the TDS for all points indicated low mineralization, according to the proposed scale by Rodier (1981). Also, according to Güler and Thyne (2004), low values in said parameters reveal that these water sampling points (classified beforehand as springs in the EIA of the GCL) are recently recharged rainwater, as there are no indicators that these are deep, intermediate, and local regional fluxes or that there is a prolonged water/rock interaction in these outcrops.

The spatial distribution of the EC in the four inventory campaigns (Figure 2) did not show a defined trend related to the altitude or the geology, nor did the regressions assessed between the EC and the OD with the elevation (Figure 3), indicating that altitude does not influence the magnitude of either parameter. That is, there is no spatial variability of these so-called springs but a temporal variability with values that will increase slightly in the more recent campaigns, which may be associated with anthropic changes in the area related, for example, to variations in land cover and land use (agriculture, forest fires, artisanal mining) and also this behaviour may also be associated with changes in precipitation, as the four sampling campaigns were carried out in different years and under different hydrological conditions. Therefore, implementing in-situ monitoring at longer intervals but over a longer time span could be an effective strategy to better understand the system's response to seasonal variability.

The preceding demonstrates that the surface unit on which most of the water sampling points (previously classified as springs) emerge (according to EIA) exhibits almost homogeneous hydrogeological behavior throughout the area. The so-called springs emerge in the first few centimeters of residual soil, saprolite, and slope deposits (vadose zone), which are part of a water transit hydrogeological unit and not of an exploitable aquifer. Therefore, the hypothesis is that most of the area's emerging water (presumed to be spring water) originates mainly from rainwater accumulation, because the mean electrical conductivity of rainfall in the study area is 50 µS/cm. In comparison, the presumed springs classified within Cluster 1 during both hydrochemical campaigns present EC values ranging from 72 to 81 µS/cm, which are relatively similar to those of rainfall.

Likewise, more than 50% of the sampling points were dry in at least one campaign; therefore, only the 100 points with continuous water flow across all four campaigns were analyzed. This fact could support the previous conclusions in the sense that most of the emerging water comes from recent recharge because these points respond very easily to rainfall and its seasonal variability since, in the area, rainfall has a high spatial variability (Integral S.A., 2015) and, being in a tropical climate, it is possible that streaks of days without rain occur in the winter time, or several rainy days could come in the summer time.

On the other hand, numerous studies have successfully used HCA, PCA, and FA to identify the sources responsible for water quality variations (Güler et al., 2002; Güler and Thyne, 2004; Singh et al., 2004; Jalali, 2006; Ragno et al., 2007; Cloutier et al., 2008; Lourenço et al., 2010; Jalali, 2016; Pazand and Javanshir, 2016; Ravikumar and Somashekar, 2017; Chen et al., 2018; Mostaza-Colado et al., 2018).

Regarding the PCA and the FA in C1-HQ, the first five factors that explain the highest data variance percentage (Table 6) and the respective principal component loads (Table 7) show that the first factor has the highest and positive loads for HCO^{3-},

SIO_2, Ca^{2+}, Mg^{2+}, K^+, which may represent a factor associated with the area's lithology due to a possible silicate alteration (andesine, orthoclase, albite biotite, and amphiboles) (Pazand and Javanshir, 2016) and as a result of dissolved CO_2 reacting with silicate minerals, cations and bicarbonate are released.

On the other hand, the second factor shows strong positive loadings for Na^+, SIO^2, and EC, indicating the possible presence of silicate alteration, such as plagioclase (andesine and albite), which releases sodium and SIO_2 and increases EC (Pazand and Javanshir, 2016). Fator 3 exhibits high positive loads for DO and negative for Fe, possibly associated with oxidation-reduction processes in the vadose zone and also this factor may also reflect the geochemical influence of the granodiorite with auriferous mineralization, where the presence of sulfide minerals such as pyrite could lead oxidation and/or progressive reduction, promoting the mobilization of Fe Tesoriero, A. J. et al (2024); Champ D.R., (1979).

Factor 4 has high positive pH loads, which govern the speciation and solubility of numerous trace elements (including Fe), and strongly influences the adsorption and ion-exchange capacity of mineral surfaces (Rabajczyk and Namieśnik, 2014; von der Heyden & Roychoudhury, 2015). In particular, as pH increases, dissolved Fe concentrations typically decrease owing to Fe hydrolysis and precipitation, consistent with a negative Fe loading in our PCA (−0.22).

Similarly, in C2-HQ, it was found that the parameters in Factor 1 with the highest and most positive loads were HCO^{3-}, Ca^{2+}, and CE, which may represent a factor associated with the area's lithology, indicating that the sampling points' EC is mainly explained by these two parameters (Pazand and Javanshir, 2016). For Factor 2, the positive loadings are associated with Na^+, K^+, HCO^{3-}, and SiO_2, which are linked to silicate alteration processes (plagioclase and orthoclase) (Jalali, 2016; Pazand and Javanshir, 2016). In Factor 3, high negative loads for Fe and positive for OD predominate, possibly associated with oxidation-reduction processes in the vadose zone. Factor 4 shows high positive loads with pH, similar to campaign 1. As pH increases, dissolved Fe concentrations typically decrease owing to Fe hydrolysis and precipitation, consistent with a negative Fe loading (−0.03).

The lines connecting the hydrochemical variables (Figures 4 and 5) indicate the contribution of these variables to the data (Ravikumar and Somashekar, 2017). The grouping of the water sampling points concerning the different ions shows that there are three similar groups in both campaigns, except for the "Aljibe 224" and “Humedal La Mayoría” surface water samples, which were not grouped in cluster 1 for C2-HQ but in cluster 2, since for that temporality, their chemistry was more alike to the alluvial piezometers. For both campaigns, the multivariate analyses revealed that, in general, the sampling points of clusters 2 and 3 are more closely correlated with the concentrations of CE, K^+, Ca^{2+}, Na+, Mg^{2+}, HCO^{3-}, SiO_2, and Fe (Figures 4 and 5). Since these elements originate from silicate alterations, these clusters indicate a greater degree of water-rock interaction. In contrast, cluster 1 is associated with pH and DO, indicative of vadose-zone processes involving organic matter oxidation and CO2 hydrolysis, which decrease pH and DO (Singh et al., 2004).

The grouping of the 21 data points using multivariate statistics revealed coherence within each cluster (e.g., spring water, alluvial or rock piezometer, surface water) and across the degree of mineralization. For instance, cluster 3 has the highest major ions and EC values and was the only one that, in both campaigns, grouped two presumed springs (M189, M121) with groundwater from alluvial and rock piezometers, revealing that some of the sampling points classified as presumed springs have origins and processes more associated with rainwater and surface water bodies. In contrast, other presumed springs originate from deeper piezometric levels or longer subsoil residence times, such as those evidenced by cluster 3.

With Piper's diagram, it is not possible to evaluate other processes that occur at each sampling point, nor to discriminate groups based on their chemistry (Güler et al., 2002), as was done previously in the statistical analysis, for which other techniques indicative of hydrochemical processes (such as the Gibbs diagram) were employed. The Gibbs diagram allows differentiation of the processes that gave rise to the water chemistry. Even though this graph was initially conceived for surface water analysis (Marandi and Shand, 2018), it has been widely used to determine the relationship between the lithological features of hydrogeological units and water composition (Kumar et al., 2009).

The diagram showed that, for both campaigns, there were two presumed springs whose primary water chemistry process was water-rock interaction. These were the M121 and M189, which, as previously seen, were grouped by multivariate statistics with groundwater (cluster 3). It is worth noting that in C2-HQ, the M219 spring was grouped in this process, whereas in C1-HQ, the same point was not associated with this field. Furthermore, according to previous statistical analysis results, its grouping cluster is associated with surface water. It is then inferred that its appearance in the water-rock interaction process reflects a temporary variation, likely related to anthropogenic contamination or to the fact that C2-HQ was conducted during the transition to the dry season, which resulted in higher ion concentrations.

Another tool to assess water hydrochemistry was the bivariate ionic relationship. Among the 13 points designated beforehand as springs by the EIA, these relationships indicated that the emerging water is associated with CO2 hydrolysis and silicate alteration in the vadose zone (Lakshmanan et al., 2003; Elango and Kannan, 2007; Kumar et al., 2009; Zhang et al., 2020). In addition, cation exchange can also occur (Lakshmanan et al., 2003; Jalali, 2007; Zhang et al., 2020). Such exchange is consistent with the bicarbonate anion presence as the dominant one at all sampling points since rainfall contains CO2(g) that, once it enters the vadose zone and reacts with the organic matter, releases more CO2(g), which, in contact with soil water, produces carbonic acid (aqueous) that, when dissociated, produces HCO3 and H+ which also allows soil mineral alteration and thus, increasing HCO3 concentration in water, especially on thick soil profiles such as those in the study area, where SiO2 is also released (Appelo and Postma, 2005).

The ionic relationship of HCO_3-+$SO4^{2-}$ vs $Ca^{2+}Mg^{2+}$ (Figure 8 and Figure 9) was evaluated, indicating a possible silicate alteration (Lakshmanan et al., 2003; Elango and Kannan, 2007; Kumar et al., 2009; Zhang et al., 2020). In this case, most of the springs were clustered slightly above or on the 1:1 stoichiometric line, suggesting that silicate alteration processes may be at work. However, there are sampling points below this line, such as M92, M79, and M74, where it is presumed that the release of bicarbonates and calcium is associated with CO2 hydrolysis by organic matter oxidation in the vadose zone.

Since practically all of the region's waters emerge at residual soils or saprolite, which have been subjected to chemical weathering for thousands of years as well as very slow degradation and mineral transformation processes (Appelo and Postma, 2005), it was also clear from the other ionic relationship diagrams (Figures 8 and 9) that silicate alteration and cation exchange are occurring in some samples. However, it was previously shown that the so-called spring points, which present these hydrochemical processes, were grouped in cluster 1 and are related to rain and surface water. This indicates that, for cation exchange or silicate alteration to occur, water does not necessarily require a long storage time for a soil/rock interaction. Still, it only requires the availability of ions associated with the geology through which the water is flowing, consistent with the abundant clay in the soil profile.

Regarding the average Stiff diagrams of clusters 1 and 2 (Figure 10), they are very similar; however, when evaluating Fe concentration, it was observed that cluster 2 has a higher Fe content than cluster 1. The oxidation-reduction reactions that release Fe occur over a long period, which explains why this variable does not appear in cluster 1, as this group would be mainly related to recent rainwater.

Finally, it was possible to classify the 13 springs on which the hydrochemical and statistical analyses for the area were focused. For two different sampling dates, 11 water sampling points can be classified as vadose water since their chemistry is very similar to that of surface and rainwater, is not well mineralized, and emerges in the first layer of saprolite, predominating in the upper and middle sections of the study area. On these points, the hydrochemical processes show an origin associated with precipitation and CO_2 hydrolysis processes in the vadose zone, which generates calcium bicarbonate waters.

On the other hand, points M121 and M189 exhibit opposite behavior, with higher ion concentrations, and are not associated with local contamination processes; their chemistry is similar to that of deep rock or alluvial piezometers. Additionally, these sampling points were grouped according to the water-rock interaction process depicted in the Gibbs diagram. Additionally, in the Stiff diagrams, both points are among the zone's most mineralized. They are located at the lowest elevations, which allows them to be classified as strictly springs for this study. Beyond the hydrochemical and statistical analyses, the correlation between rainfall EC data and the presumed springs enabled the identification of those springs most strongly influenced by precipitation.

A limitation of this study is that the water spring classification did not consider factors such as vegetation cover, multitemporal vegetation cover analyses, and land use, which are other characteristics that can help define and classify springs. Another limitation is the availability of data for all the analyses carried out, as this information in Colombia is restricted to private studies that become public domain once the environmental licenses are obtained.

This study has achieved a preliminary technical classification of water outcrops, supported by several areas of knowledge, which enables the protection of the water resource and also defines the cases in which the soil can be used for purposes other than protection without detriment to this vital natural resource. These kinds of studies are crucial for the region's economic progress, not only from an extractive approach, such as mining, but also from the energy, environmental, and infrastructure perspectives required for the sustainable development of a country like Colombia.

6. CONCLUSIONS

This study proposes a methodology for classifying water sampling points between springs or vadose water discharges using multivariate cluster and hydrogeochemical techniques. We

verified that the interplay between hydrogeochemical techniques and statistical results enables highly consistent classification of the emerging water type based on its origins and processes.

In the study area, there are no exploitable regional or local aquifers. However, there is evidence of a hydrogeological unit of transit water, within which numerous water-emerging points can be found and classified as vadose water, which discharges onto the ground and has a rainwater-like physicochemical composition. It was also possible to verify that deep zones associated with the weathering profile and fresh rock can serve as groundwater storage, resulting in water outcrops with longer water-rock interaction times, which were strictly classified as springs.

The next step in this research is to conduct the same analyses using more extensive data across various lithologies and hydrogeological contexts to verify whether springs can be classified using multivariate statistics and hydrogeochemistry, as presented here.

ACKNOWLEDGMENTS

We gratefully acknowledge Gramalote Colombia Limited for granting access to the data used in this study.

CONFLICT OF INTEREST

The authors declare that they have no conflicts of interest related to the publication of this paper.

7. REFERENCES

Appelo, C.A.J.; Postma, D. (2005). Geochemistry, groundwater and pollution. 2nd ed. CRC Press. https://doi.org/10.1201/9781439833544

Champ, D.R; J. Gulens, J; Jackson R. E. . 1979. Oxidation–reduction sequences in ground water flow systems. Canadian Journal of Earth Sciences. 16(1): 12-23. https://doi.org/10.1139/e79-002

Chen, T.; Zhang, H.; Sun, C.; Li, H.; Gao, Y. (2018). Multivariate statistical approaches to identify the major factors governing groundwater quality. Applied Water Science, 8(7), 1–6. https://doi.org/10.1007/s13201-018-0837-0

Cloutier, V.; Lefebvre, R.; Therrien, R.; Savard, M.M. (2008). Multivariate statistical analysis of geochemical data as indicative of the hydrogeochemical evolution of groundwater in a sedimentary rock aquifer system. Journal of Hydrology, 353(3–4), 294–313. https://doi.org/10.1016/j.jhydrol.2008.02.015

Custodio, E.; Llamas, M. (1975). Hidrología subterránea. Barcelona: Editorial Omega, vol. 2.

Davis, J. (1986). Statistics and data analysis in Geology. New York: John Wiley and Sons, Inc.

De la Fuente, S. (2011). Análisis de correspondencias simples y múltiples. Facultad de Ciencias Económicas y Empresariales Universidad Autónoma de Madrid. https://www.fuenterrebollo.com/Economicas/ECONOMETRIA/REDUCIR-DIMENSION/CORRESPONDENCIAS/correspondencias.pdf

Doménico, P., & Schawartz, F. (1997). Physical and Chemical Hydrogeology. New York, USA.: John Wiley E Sons, Inc.

Elango, L.; Kannan, R. (2007). Chapter 11 Rock-water interaction and its control on chemical composition of groundwater. Developments in Environmental Science, 5(07), 229–243. https://doi.org/10.1016/S1474-8177(07)05011-5

Freeze, R.; Cherry, J. (1979). Groundwater. N.J: Prentice-Hall.

Gibbs, R. (1970). Mechanisms controlling world water chemistry. Science, New Series, Vol. 170, (3962), 1088-1090. https://doi.org/10.1126/science.170.3962.1088

Golder Associates (2014). Evaluación hidrogeológica. Documento soporte para la EIA. Medellín.Colombia

Güler, C.; Thyne, G.; McCray, J.; Turner, A. (2002). Evaluation of graphical and multivariate statistical methods for classification of water chemistry data. Hydrogeology Journal, 10(4), 455–474. https://doi.org/10.1007/s10040-002-0196-6

Güler, C.; Thyne, G.D. (2004). Hydrologic and geologic factors controlling surface and groundwater chemistry in Indian Wells-Owens Valley area, southeastern California, USA. Journal of Hydrology, 285(1–4), 177–198. https://doi.org/10.1016/j.jhydrol.2003.08.019

Hounslow, A. (1995). Water quality data: analysis and interpretation. Boca Raton. CRC Press LLC, Lewis Publishers

ICONTEC (2014). Guía técnica colombiana GTC-ISO 30. Bogotá: Instituto Colombiano de Normas Técnicas y Certificación (ICONTEC)

Integral S.A. (2015). Estudio de impacto Ambiental proyecto de minería de oro a cielo abierto Gramalote. Medellín. Colombia.

Instituto de Hidrología, Meteorología y Estudios Ambientales – IDEAM (2021). Consulta y descarga de datos hidrometeorológicos. Disponible en http://dhime.ideam.gov.co/atencionciudadano/. Recovered 05-11-2022.

Jalali, M. (2006). Chemical characteristics of groundwater in parts of mountainous region, Alvand, Hamadan, Iran. Environmental Geology, 51(3), 433–446. https://doi.org/10.1007/s00254-006-0338-6

Jalali, M. (2007). Assessment of the chemical components of Famenin groundwater, western Iran. Environmental Geochemistry and Health, 29(5),357–374. https://doi.org/10.1007/s10653-006-9080-y

Jalali, M. (2016). Geochemistry and background concentration of major ions in spring waters in a high-mountain area of the Hamedan (Iran). Journal of Geochemical Exploration. 165, 49–61. https://doi.org/10.1016/j.gexplo.2016.02.002

Kumar, S.K.; Rammohan, V.; Sahayam, J.D.; Jeevanandam, M. (2009). Assessment of groundwater quality and hydrogeochemistry of Manimuktha River basin, Tamil Nadu, India. Environmental Monitoring and Assessment, 159(1–4), 341–351. https://doi.org/10.1007/s10661-008-0633-7

Lakshmanan, E.; Kannan, R.; Senthil Kumar, M. (2003). Major ion chemistry and identification of hydrogeochemical processes of ground water in a part of Kancheepuram district, Tamil Nadu, India. Environmental Geosciences, 10(4), 157–166. https://doi.org/10.1306/eg.0820303011

Lourenço, C.; Ribeiro, L; Cruz, J. (2010). Classification of natural mineral and spring bottled waters of Portugal using Principal Component Analysis. Journal of Geochemical Exploration, 107, 362–372. https://doi.org/10.1016/j.gexplo.2010.08.001

Malagón, J.P.; Piña, A.; Argüello, S; Donado, L.D. (2021). Análisis hidrogeoquímico multivariado del agua subterránea del sistema acuífero del Valle Medio del Magdalena, Colombia: Estudio a escala regional. Boletín de la Sociedad Geológica Mexicana, 73(3), A070421. http://dx.doi.org/10.18268/BSGM2021v73n3a070421

Marín, J.M. (2021). Estadística descriptiva y análisis de datos.Tema 4: Transformaciones de variables. Available in: http://halweb.uc3m.es/esp/Personal/personas/jmmarin/esp/EDescrip/tema4.pdf. Recovered: 06-05-2021

Marandi, A.; Shand, P. (2018). Groundwater chemistry and the Gibbs diagram. Applied Geochemistry, 97, 209–212. https://doi.org/10.1016/j.apgeochem.2018.07.009

Mazor, E. (2003). Chemical and isotopic groundwater hydrology. 3rd edition. CRC Press

Minitab Inc. State (2021). Minitab Release 14®. (C. Pensilvania, Ed.) EE. UU.

Mostaza-Colado, D.; Carreño-Conde, F.; Rasines-Ladero, R.; Iepure, S. (2018). Hydrogeochemical characterization of a shallow alluvial aquifer: 1 baseline for groundwater quality assessment and resource management. Science of the Total Environment, 639, 1110–1125. https://doi.org/10.1016/j.scitotenv.2018.05.236

Pazand, K., Javanshir, A.R. (2016). Application of multivariate statistical techniques in hydrogeochemical evolution of groundwater in an igneous rock and sedimentary aquifer system: a case study of the southern Bam, SE Iran. Carbonates and Evaporites, 31(1), 9–16. https://doi.org/10.1007/s13146-015-0234-9

Piper, A.M. (1944). A graphic procedure in the geochemical interpretation of water-analyses. Eos, Transactions American Geophysical Union, 25(6), 914-928. https://doi.org/10.1029/TR025i006p00914

Ragno, G.; De Luca, M.; Ioele, G. (2007). An application of cluster analysis and multivariate classification methods to spring water monitoring data. Microchemical Journal, 87(2), 119–127. https://doi.org/10.1016/j.microc.2007.06.003

Rabajczyk, A.; Namieśnik, J. (2014). Speciation of Iron in the Aquatic Environment. Water Environment Research, 86(8), 741–758. http://www.jstor.org/stable/24585466

Ravikumar, P.; Somashekar, R.K. (2017). Principal component analysis and hydrochemical facies characterization to evaluate groundwater quality in Varahi river basin, Karnataka state, India. Applied Water Science, 7, 745–755. https://doi.org/10.1007/s13201-015-0287-x

Rodier, J. (1981). Análisis de las aguas. Barcelona: Omega.

Redlands, C. E. S. R. I. (2011). ESRI 2011. ArcGIS Desktop: Release 10

Singh, K.P.; Malik, A.; Mohan, D.; Sinha, S. (2004). Multivariate statistical techniques for the evaluation of spatial and temporal variations in water quality of Gomti River (India) - A case study. Water Research, 38(18), 3980–3992. https://doi.org/10.1016/j.watres.2004.06.011

Simler, R. (2021). Logiciel d'hydrochimie- Water Software Quality Hydrochemistry diagrams, DIAGRAMMES: http://www.lha.univ-avignon.fr/LHA-Logiciels.htm. Recovered 14-11-2021

Springer, A.; Stevens., L. (2008). Spheres of discharge of springs. Hydrogeology Journal, 17, 11. https://doi.org/10.1007/s10040-008-0341-y

Stevens, L.; Ledbetter, J.; Springer, A. (2012). Springs inventory and assessment training manual, Version 2.01. Springs Stewardship Institute, Museum of Northern Arizona, Flagstaff. Obtenido de http://springstewardship.org/workshops.html Recovered 18-11-2021

Swan, A.; Sandilands, M. (1995). Introduction to geological data analysis. Oxford: Blackwell Science: Blackwell Science.

Tesoriero, A. J.; Wherry, S. A.; Dupuy, D. I.; Johnson, T. D. (2024). Predicting Redox Conditions in Groundwater at a National Scale Using Random Forest Classification. Environmental Science & Technology,58(11),5079-5092. https://doi.org/10.1021/acs.est.3c07576pubs.acs.org+2pubmed.ncbi.nlm.nih.gov+2

Toro, M.T. (2020). Groundwater resources of the western Andean front: insights from the Aconcagua basin, central Chile. Tesis para optar al grado de doctor en ciencias mención geología. Santiago de Chile: Universidad de Chile. https://repositorio.uchile.cl/bitstream/handle/2250/176630/Groundwater-resources-of-the-Western-Andean-Front-insights-from-the-Aconcagua-Basin.pdf?sequence=1&isAllowed=y

Zhang, B.; Zhao, D.; Zhou, P.; Qu, S.; Liao, F.; Guangcai, W. (2020). Hydrochemical characteristics of groundwater and dominant water – rock interactions in the Delingha Area, Qaidam Basin, Northwestern China. Water, 12(836), 1–16. https://doi.org/10.3390/w12030836.

Von der Heyden, B. P.; Roychoudhury, A. N. (2015). Application, chemical interaction and fate of iron minerals in polluted sediment and soils. Current Pollution Reports, 1, 265–279. https://doi.org/10.1007/40726-015-0020-2